Published in final edited form as:
Ophthalmic Genet. 2014 September ; 35(3): 142–150. doi:10.3109/13816810.2014.915328.

Next-generation Sequencing Revealed a Novel Mutation in the Gene Encoding the Beta Subunit of Rod Phosphodiesterase

Sherry Shen[1], **Tharikarn Sujirakul**[2,3], and **Stephen H. Tsang**[2,4,5]

[1]College of Physicians & Surgeons, Columbia University, New York, NY, USA [2]Edward S. Harkness Eye Institute, Columbia University, New York, NY, USA [3]Department of Ophthalmology, Ramathibodi Hospital, Mahidol University, Bangkok, Thailand [4]Bernard & Shirlee Brown Glaucoma Laboratory, Departments of Ophthalmology, Pathology & Cell Biology, Columbia University, New York, NY, USA [5]New York-Presbyterian Hospital/Columbia University Medical Center, New York, NY, USA

Abstract

Purpose—To report the phenotypes caused by a novel mutation in the *PDE6B* gene in a family with two affected siblings and one affected cousin with a 2-year follow-up.

Design—Three patients from a family with a history of retinitis pigmentosa underwent clinical evaluations. The affected patients' DNA was analyzed using next-generation sequencing and segregation analyses were performed for the family.

Setting—Edward S. Harkness Eye Institute, New York Presbyterian Hospital.

Participants—Two siblings, one cousin, and five unaffected family members.

Main outcome measures—Macular appearance assessed by funduscopy, autofluorescence imaging, spectral-domain optical coherence tomography and visual function assessed by electroretinography.

Results—The proband, brother, and cousin had rod-cone degeneration with cystoid macular edema. Fundus autofluorescence showed hyperautofluorescent ring constriction over time. Spectral-domain optical coherence tomography revealed retinal pigment epithelium atrophy, loss of external limiting membrane, retinal layer thinning, and reduction in ellipsoid zone length over time. Next-generation whole exome sequencing revealed a homozygous c.1923_1969ins6del47 nonsense *PDE6B* mutation, which has not been previously described, that segregated with the disease in the family.

Conclusions—The homozygous *PDE6B* mutation causes retinitis pigmentosa. Acetazolamide treatment improved visual acuity but rod degeneration continued. Despite having the same

Correspondence: Stephen H. Tsang, Edward S. Harkness Eye Institute, New York-Presbyterian/Columbia University Medical Center, 160 Fort Washington Avenue, Research Annex, Room 513, New York, NY 10032, USA. Tel: +001 212 3421189; Fax: +001 212 3054987. sht2@columbia.edu.

DECLARATION OF INTEREST

The authors report no conflicts of interest. The authors alone are responsible for the content and writing of the paper.

mutation and living in the same environment, the proband's brother progressed at a faster rate starting at a younger age, suggesting that gene modifiers may influence the expressivity of the phenotype. Next-generation sequencing, used to discover this mutation, is a practical new technology that can detect novel disease-causing alleles, where previous arrayed primer extension (APEX) technology could not.

Keywords

Fundus autofluorescence; next-generation sequencing; optical coherence tomography; PDE6; retinitis pigmentosa; rod phosphodiesterase; whole exome sequencing

INTRODUCTION

Retinitis pigmentosa (RP) is a heterogeneous neurodegenerative disease characterized by photoreceptor death and progressive vision loss that affects one in 3000 people and a total of 1.5 million worldwide.[1] Patients with RP typically present with symptoms of night blindness from rod degeneration and central vision loss from cone degeneration, eventually experiencing complete loss of vision. Other clinical features of RP include waxy, pale optic disc, attenuated arterioles, and bone spicule pigmentation.[2] More than 35 genes have been associated with autosomal recessive RP (arRP), the most common type of inheritance pattern in this disease (www.sph.uth.tmc.edu/Retnet/sum-dis.htm#B-diseases). It is estimated that 10% of Americans carry a mutation in one of those genes.[1,3]

About 36,000 arRP cases (8%) are due to defects in rod-specific cyclic guanosine monophosphate (cGMP) phosphodiesterase 6 (PDE6).[4,5] When light strikes the photoreceptor, rhodopsin activates transducin *GNAT1*, which binds the two regulatory PDE6γ subunits.[6] The catalytic PDE6α and β subunits are then activated to hydrolyze cGMP, resulting in the closing of ion channels and membrane hyperpolarization.[7] In *rd1* mouse models, mutations in the *PDE6B* homolog have been shown to cause inherited retinal degeneration.[8,9] However, the mechanisms by which defective PDE6 leads to the rod and cone degeneration of RP remain unclear.

The *PDE6B* gene (MIM# 613801) maps to chromosome 4p16.3 and has 22 exons, translating to the PDE6β subunit; mutations in this gene are associated with retinitis pigmentosa type 40 and congenital stationary night blindness.[10–12] Various arRP-associated mutations in the *PDE6B* gene have been described.[4,5,12–19] These patients were reported to have clinical findings typical of RP, including decreased night vision starting in early childhood, elevated dark adapted thresholds, attenuated arterioles, and bone spicule pigment around the midperipheral retina; many patients showed preserved visual acuity until late disease stages (best corrected visual acuity of 20/40 or better) and some had posterior subcapsular cataracts.[12,13,15]

Although many patients with *PDE6B* mutations have been identified and exhibit typical findings of autosomal recessive RP on clinical exam and ophthalmoscopy, few have been followed long-term by multiple imaging modalities. Here we report the identification and 2-year follow-up of a novel homozygous *PDE6B* mutation in two affected brothers and their cousin and present their unique phenotypes through color fundus photographs, fundus

autofluorescence (FAF), and spectral domain optical coherence tomography (SD-OCT). Due to the heterogeneity of RP, it is important to establish characteristic genotype-phenotype correlations in the various autosomal recessive RP-associated genes. In forms of RP that do not show good genotype-phenotype correlation, next-generation sequencing (NGS), employed in this study, can identify novel causative mutations.

MATERIALS AND METHODS

Patients and Clinical Evaluation

The proband, his affected brother, their affected cousin, three unaffected siblings, and parents were enrolled in the study under protocol #AAAB6560 after obtaining full consent. The Institutional Review Board at Columbia University has approved the protocol and this study is in accordance with HIPAA regulations.

Each patient received a complete clinical evaluation by a retinal physician (S.H.T.). Color fundus photography was performed using a FF 450plus Fundus Camera (Carl Zeiss Meditec AG, Jena, Germany). Fundus autofluorescence images were acquired by confocal scanning-laser ophthalmoscope (Heidelberg Retina Angiograph 2, Heidelberg Engineering, Dossenheim, Germany), using an argon laser light (488 nm) to illuminate the fundus and a band pass filter with a short wavelength cut-off at 495 nm AF to view the resultant fluorescence.[20–25] SD-OCT images were obtained using a confocal scanning laser ophthalmoscope (Spectralis HRA-OCT; Heidelberg Engineering, Heidelberg, Germany). Ring diameter in FAF and width of inner segment ellipsoid zone in SD-OCT were measured using Heidelberg Eye Explorer software by two independent graders and averaged. Diagnosys Espion Electrophysiology System (Diagnosys LLC, Littleton, MA, USA) was used to perform electroretinography (ERG). For all recordings, tropicamide (1%) and phenylephrine hydrochloride (2.5%) were used to maximally dilate pupils before full-field ERG testing and a drop of 0.5% proparacaine was used to anesthetize the corneas. Full-field ERGs were performed using silver impregnated fiber electrodes (DTL; Diagnosys LLC, Littleton, MA) with a ground electrode on the forehead, and extended testing protocols were in accordance with the International Society for Clinical Electrophysiology of Vision (ISCEV) standard.

Genetic Analyses

The proband, his brother, and their cousin underwent next-generation whole exome sequencing and the rest of the family was subjected to co-segregation analysis. After obtaining consent from the proband, brother, and cousin, blood was drawn and 3–5 micrograms of DNA were extracted, exome captured, and sequenced at Ambry Genetics (Aliso Viejo, California). Nimblegen capture array (SeqCap EZ Exome Library v3.0) was used to perform in-solution sequence capture and Illumina HiSeq platform with 100-base paired end reads was used for massively parallel sequencing. Instrument-specific Real Time Analysis software was used for nucleotide calling and quality score assessment, then sequencing reads in fastq format were generated. Burrows-Wheeler Aligner was used to align the read pairs to a human reference genome (hg19) and PICARD tools were used to eliminate duplicate reads. Samtools were used for in/del and SNP calling after on-target

reads were extracted. ANNOVAR was used to annotate variants, which were confirmed by Sanger sequencing. The results were filtered based on the autosomal recessive inheritance pattern in the family.

RESULTS

Clinical Examination

The proband is a 22-year-old man who experienced the onset of blurry vision and nighttime vision deficiency at age 9 and was diagnosed with retinitis pigmentosa at age 17. The brother of the proband is a 15-year-old boy who presented with similar symptoms at age 10. The family, of Egyptian Sephardic Jewish descent, includes three other siblings and parents who have no history of RP or other eye diseases (Figure 1). The mother and father of the proband are first cousins; FAF and OCT images from both parents revealed no retinal abnormalities. Their mutual first cousin was diagnosed with RP around age 40. A mutual aunt also had an eye disease, but limited information is available about her diagnosis. The cousin of the proband is a 21-year-old man who presented with symptoms of RP at age 9 and was formally diagnosed at age 11. He is the son of the proband's maternal uncle (Figure 1). The cousin's parents are also consanguineous. There was no other history of hearing loss, birth defects, or intellectual disability in the extended family.

The demographic and clinical findings from the proband, his brother, and their cousin are summarized in Table 1. The best corrected visual acuity (BCVA) in the proband on the first visit in May 2011 was 20/60 in both eyes (OU). His symptoms included blurry vision, increasingly deteriorating night vision, flashes, floaters, migraines, eye pain, and sensitivity to light. The anterior segment exam was normal; the dilated exam showed the presence of posterior subcapsular cataracts. Color fundus photographs show attenuated arterioles, dull foveal light reflexes, and peripheral bone spicules consistent with intraretinal pigment migration (Figure 2A & B). Cystoid macular edema (CME) is evident to a greater extent in the right eye (OD) than the left eye (OS). The optic disc shows minimal temporal pallor and there are optic nerve head drusens in both eyes. He had reduced and delayed full-field ERG with extinguished rod scotopic and maximal ERG responses and severely reduced amplitude in 30-Hz flicker. He was taking 250 mg valproic acid 3 times per day and on the first visit was prescribed 500 mg acetazolamide per day. On a follow-up visit 2 years later in March 2013, his BCVA was 20/30 in both eyes.

The proband's younger brother presented with symptoms of difficulty with night vision and blurry vision, and the clinical findings were similar. His BCVA was 20/30 in both eyes on first visit in August 2012. The anterior segment exam was normal. Color fundus photographs also show attenuated arterioles, dull foveal light reflexes, and peripheral bone spicules (Figure 2C & D). He had severely reduced and delayed full-field ERG with extinguished rod scotopic and maximal ERG responses and severely reduced amplitude in 30-Hz flicker. He was taking 250 mg valproic acid per day and was prescribed 500 mg acetazolamide per day. On a follow-up visit 1 year later in July 2013, the BCVA was 20/20 OD, 20/25 OS.

The cousin's BCVA was 20/80 OD and $20/60^{-1}$ OS on first visit in September 2010; he presented with worsening peripheral vision and had a history of seeing floaters and flashes in both eyes. ERG showed similar findings as in the proband and the brother. The cousin was taking 250 mg valproic acid per day, but reported noncompliance. On his follow-up visit 3 years later in October 2013, his BCVA had improved to $20/25^{+2}$ OU. He was prescribed 100 mg methazolamide per day.

Fundus Autofluorescence (FAF)

In the FAF images of the proband, CME and surrounding hyperautofluorescent ring are evident in both eyes (Figure 3A & D). Peripherally, there is clumping of hypoautofluorescent patches corresponding to areas of RPE atrophy seen in the color photographs. The optic disc drusen seen in the color fundus photographs are confirmed by hyperautofluorescence in the FAF images. Hyperautofluorescent ring was measured at the outer border; on first exam in May 2011, the horizontal and vertical ring diameter was 3120 and 2424 μm respectively in the right eye (Figure 3A) and 2869 and 2400 μm in the left eye (not shown). At a 2-year follow-up visit in March 2013, the ring constricted to a horizontal and vertical ring diameter of 2815, 2110 μm respectively in the right eye (Figure 3D) and 2565, 2215 μm in the left (not shown).

FAF images of the affected brother show similar findings. There is a more prominent petalloid hyper-autofluorescence pattern in the fovea suggesting CME (Figure 3B & E). At the first visit in August 2012, the brother had a smaller hyperautofluorescent ring than the proband, with horizontal and vertical ring diameter measurements of 2540, 1882 μm respectively in the right eye (Figure 3B) and 2475, 1890 μm in the left (not shown). At a 1-year follow-up visit in July 2013, the hyperautofluorescent ring showed marked constriction. The new ring measurements in the right eye at this time were 2379 and 1699 μm in the horizontal and vertical diameter in the right eye (Figure 3E) and 2374, 1767 μm in the left (not shown).

FAF images of the cousin are similar to the proband's and brother's (Figure 3C & F). At the first visit in September 2010, the hyperautofluorescent ring had horizontal and vertical diameter measurements of 2374, 1896 μm in the right eye (Figure 3C) and 2774, 2124 μm in the left (not shown). At the 3-year followup visit in October 2013, the ring had constricted to horizontal and vertical diameters of 2249, 1749 μm in the right eye (Figure 3F) and 2493, 2001 μm in the left (not shown).

Spectral Domain-Optical Coherence Tomography (SD-OCT)

The proband's SD-OCT images show peripheral RPE thinning and loss of ellipsoid and external limiting membrane (Figure 4A & B). There is pronounced retinal layer thinning in the outer nuclear layer and a loss of foveal contour in both eyes. Cysts are present in the outer and mostly inner plexiform layers, and there is thinning of the outer plexiform layer. Inner segment ellipsoid zone in the right eye had a length of 1771 μm on first visit; at the 2-year follow-up visit, the length had decreased to 1635 μm (Figure 4A & B). The left eye showed similar measurements: 1809 μm on first visit decreasing to 1644 μm on follow-up (not shown).

The affected brother's SD-OCT images are similar, showing peripheral RPE atrophy and thinning of the retinal layer (Figure 4C & D). There is a loss of external limiting membrane and thinning of the outer nuclear layer outside the area of ellipsoid preservation. The cysts are present only in the internal plexiform layer. Ellipsoid zone preservation area is shorter in length than the proband's at first exam at 1361 μm in the right eye (Figure 4C) and 1158 μm in the left (not shown). The line showed marked reduction in length at the 1-year follow-up visit to 1232 μm in the right eye (Figure 4D) and 1051 μm in the left, more severe than in the proband.

The cousin's SD-OCT images are similar to the proband's and brother's (Figure 4E & F). The ellipsoid zone constricted in length over time from 1458 μm in the right eye (Figure 4E) and 1896 μm in the left to 1416 μm in the right eye (Figure 4F) and 1575 μm in the left on follow-up exam 3 years later in October 2013.

Genetic Analyses

The proband, his brother, and their cousin underwent next-generation sequencing. The results were filtered based on the autosomal recessive inheritance pattern of the family. Based on the candidate genes' functions and the nature of the alterations, a single notable homozygous mutation c.1923_1969ins6del47 (p.T641TfsX31) in the *PDE6B* gene was identified in the proband, brother, and cousin. This mutation, present in exon 16, consists of a frameshift at amino acid position 641 resulting in a premature stop codon. The unaffected mother, father, two sisters and brother are all heterozygous carriers of this mutation.

DISCUSSION

This case report presents the clinical and genetic findings of a proband, his affected brother, and their affected cousin in a consanguineous family with a homozygous c. 1923_1969ins6del47 (p.T641TfsX31) *PDE6B* mutation, which has not been previously reported. This mutation consists of a 47-bp insertion and 6-bp deletion resulting in a frameshift at amino acid position 641 and a premature stop codon. The truncated protein results in the loss of exons 16–22, interrupting the catalytic region for cGMP hydrolysis located at amino acid positions 555–792.[26] The premature stop codon likely results in a nonfunctional PDE6β and high levels of cGMP, leading to decreased ion channel closure and ultimately, lower levels of photoreceptor hyperpolarization and signaling in response to light stimulation. Although the mechanism by which deficient PDE6β leads to RP disease remains unclear, one hypothesis suggests that increased Ca^{2+} influx from decreased channel closure leads to rod degeneration and apoptosis.[27,28]

Various *PDE6B* mutations, including C270X, Q298X, P496(1-bp del), L527P, R531X, H557Y, G576D, H620(1-bp del), K706X, L854V, W807R, I535N, R552Q, P387L, D600N have been reported to cause retinitis pigmentosa.[4,5,12–19,29,30] The clinical phenotypes in these cases are consistent with typical findings in RP: early childhood onset of night vision loss, attenuated retinal vessels and bone spicule pigment on ophthalmoscopy, elevated dark adapted threshold, and generally well-preserved visual acuity until late stages. The symptoms and clinical findings in the proband, brother, and cousin are generally consistent with what has been reported in other PDE6β-deficient patients. There appears to be no

particularly unique phenotype associated with premature termination mutations, or with mutations affecting the catalytic domain of *PDE6B*.[5,15] Jacobson and colleagues reported evidence of retinal thickening along the arcades and thinning in the parafoveal region in a PDE6β-deficient patient with a C270X mutation, but this retinal remodeling was not evident in the present case.[30]

FAF images of the proband, brother, and cousin showed hyperautofluorescent ring formations. Hyperautofluorescent ring has been described in RP patients; hypoautofluorescent areas outside the ring are associated with RPE degeneration, while the ring is associated with lipofuscin accumulation and increased RPE metabolism before the onset of photoreceptor apoptosis.[31] In RP patients, the ring constricts over time as rod photoreceptors are lost.[32,33] At first exam, the proband's brother, who is much younger in age, had a smaller ring than the other two patients, suggesting greater photoreceptor loss. The proband's follow-up exam was two years after the first exam; in that time the rate of ring constriction per year was 167 μm and 171 μm in the horizontal and vertical diameters in the right eye respectively and 166 μm and 101 μm in the left eye. The brother's follow-up exam was 1 year after first exam. His rate of ring constriction per year was 176 μm and 200 μm in the horizontal and vertical diameters in the right eye and 110 μm and 134 μm in the left. The cousin's follow-up exam was 3 years after first exam; his rate of ring constriction per year was 42 μm and 49 μm in the horizontal and vertical diameters respectively in the right eye and 94 μm and 41 μm in the left. The younger brother showed a greater rate of ring constriction than the proband and cousin in all parameters except horizontal diameter in the left eye. In the proband and brother, progression in the right eye was faster.

Shortening of the inner segment ellipsoid zone on SD-OCT has been correlated with decreased retinal sensitivity in RP patients.[34] SD-OCT in this case showed smaller preservation of the ellipsoid zone over time in both the proband and the affected brother. The proband's rate of ellipsoid zone shortening over time was 74 μm per year in the right eye and 90 μm in the left, the brother's rate was 140 μm per year in the right eye and 116 μm in the left, and the cousin's rate was 14 μm in the right eye and 107 μm in the left. The brother's rate of ellipsoid zone shortening was almost twice as fast the proband's, and 10 times faster than the cousin's in the right eye. This suggests that the brother's disease started at a worse baseline and progressed faster than the proband's despite having the same mutation, based on SD-OCT. In the proband and brother, both eyes show a similar degree of progression while in the cousin, the left eye progressed faster than the right.

After the initial visit for both the proband and his affected brother, 500 mg acetazolamide per day was prescribed for both patients. The proband's BCVA improved from 20/60 OU to 20/30 OU, and the brother's BCVA improved from 20/30 OU to 20/20 OD, 20/25 OS. CME appears to have improved on SD-OCT in both patients (Figure 4). Treatment with the carbonic anhydrase inhibitor acetazolamide has been linked to improved visual acuity and decreased macular edema in patients with retinitis pigmentosa.[35] However, FAF and SD-OCT images from the proband and his brother revealed that the disease progressed and RPE degeneration continued, as measured by hyperautofluorescent ring constriction and inner segment ellipsoid zone length reduction.

The c.1923_1969ins6del47 mutation manifests with variable severity in this family. The younger affected brother had a smaller hyperautofluorescent ring and smaller preserved ellipsoid zone on SD-OCT at an earlier age, suggesting his disease is more advanced than the proband's. He also showed faster progression in ellipsoid zone shortening in both eyes and ring constriction in one eye than the proband. Since both patients have the same homozygous mutation and live in the same environment, there may be other gene modifiers that cause the younger brother to progress faster starting at a younger age. His prognosis is more severe and he should be followed closely to monitor the status of his disease.

Arrayed primer extension (APEX) technology is a widely applied diagnostic test for allelic and genetically heterogeneous diseases; however, novel variants are not detected by this method. Next-generation whole exome sequencing (NGS), which screens the entire protein coding region of the genome, is able to identify novel disease-associated alleles where APEX technology cannot; this is particularly useful in RP, a genetically heterogeneous disease. In RP, the huge potential and clinical applicability of NGS has only recently begun to be utilized in the identification of inherited and de novo mutations.[36,37] It has been estimated that NGS can successfully detect approximately 57–64% of disease-causing mutations in RP, a significant increase from the 11% diagnostic yield of APEX technology.[38–40] In this study, we used next-generation whole exome sequencing of the affected siblings and segregation analysis of the rest of the family. NGS is practical, feasible, and yields accurate results. This study supports the use of NGS technology as the method of choice in identifying the causative gene mutations in patients with RP.

In conclusion, this report describes a novel homozygous c.1923_1969ins6del47 nonsense *PDE6B* mutation, identified by next-generation whole exome sequencing, in a consanguineous family causing autosomal recessive RP. Defining genotype-phenotype correlations in autosomal recessive RP will aid in directed gene screening; however, in cases where the disease-associated gene mutation cannot be deduced from the phenotype, next-generation sequencing should be the method of choice for identifying disease-causing mutations in preparation for upcoming gene-specific treatment trials.

Acknowledgments

The Bernard & Shirlee Brown Glaucoma Laboratory is supported by NIH core grants 5P30CA013696 and 5P30EY019007, and unrestricted funds from Research to Prevent Blindness, New York, NY, USA. S.H.T. is a member of the RD-CURE Consortium and is supported by Tistou and Charlotte Kerstan Foundation, NIH R01EY018213, the Research to Prevent Blindness Physician-Scientist Award, the Barbara and Donald Jonas Family Fund, the Schneeweiss Stem Cell Fund, New York State (N09G-302), the Foundation Fighting Blindness New York Regional Research Center Grant (C-NY05-0705-0312), the Joel Hoffman Fund, Gale and Richard Siegel Stem Cell Fund, Charles Culpeper Scholarship, Irma T. Hirschl Charitable Trust, Bernard and Anne Spitzer Stem Cell Fund, Professor Gertrude Rothschild Stem Cell Foundation, and Gebroe Family Foundation. Financial support for S.S. from NHLBI (5T35HL007616-33) and Fight for Sight is gratefully acknowledged. T.S. was supported by Foundation Fighting Blindness grant CF-CL-0613-0614-COLU.

References

1. Bird AC. Retinal photoreceptor dystrophies LI. Edward Jackson Memorial Lecture. Am J Ophthalmol. 1995; 119:543–562. [PubMed: 7733180]
2. Heckenlively JR, Yoser SL, Friedman LH, Oversier JJ. Clinical findings and common symptoms in retinitis pigmentosa. Am J Ophthalmol. 1988; 105:504–511. [PubMed: 3259404]

3. Rivolta C, Sharon D, DeAngelis MM, Dryja TP. Retinitis pigmentosa and allied diseases: numerous diseases, genes, and inheritance patterns. Human Mol Genet. 2002; 11:1219–1227. [PubMed: 12015282]
4. Dryja TP, Rucinski DE, Chen SH, Berson EL. Frequency of mutations in the gene encoding the alpha subunit of rod cGMP-phosphodiesterase in autosomal recessive retinitis pigmentosa. Invest Ophthalmol Vis Sci. 1999; 40:1859–1865. [PubMed: 10393062]
5. McLaughlin ME, Ehrhart TL, Berson EL, Dryja TP. Mutation spectrum of the gene encoding the beta subunit of rod phosphodiesterase among patients with autosomal recessive retinitis pigmentosa. Proc Nat Acad Sci USA. 1995; 92:3249–3253. [PubMed: 7724547]
6. Stryer L. Cyclic GMP cascade of vision. Ann Rev Neurosci. 1986; 9:87–119. [PubMed: 2423011]
7. Cote RH. Characteristics of photoreceptor PDE (PDE6): similarities and differences to PDE5. Int J Impotence Res. 2004; 16:S28–S33.
8. Bowes C, Li T, Danciger M, et al. Retinal degeneration in the rd mouse is caused by a defect in the beta subunit of rod cGMP-phosphodiesterase. Nature. 1990; 347:677–680. [PubMed: 1977087]
9. Lem J, Flannery JG, Li T, et al. Retinal degeneration is rescued in transgenic rd mice by expression of the cGMP phosphodiesterase beta subunit. Proc Nat Acad Sci USA. 1992; 89:4422–4426. [PubMed: 1350091]
10. Altherr MR, Wasmuth JJ, Seldin MF, et al. Chromosome mapping of the rod photoreceptor cGMP phosphodiesterase beta-subunit gene in mouse and human: tight linkage to the Huntington disease region (4p16.3). Genomics. 1992; 12:750–754. [PubMed: 1315306]
11. Tsang SH, Woodruff ML, Jun L, et al. Transgenic mice carrying the H258N mutation in the gene encoding the beta-subunit of phosphodiesterase-6 (PDE6B) provide a model for human congenital stationary night blindness. Human Mutat. 2007; 28:243–254.
12. McLaughlin ME, Sandberg MA, Berson EL, Dryja TP. Recessive mutations in the gene encoding the beta-subunit of rod phosphodiesterase in patients with retinitis pigmentosa. Nature Genet. 1993; 4:130–134. [PubMed: 8394174]
13. Bayes M, Giordano M, Balcells S, et al. Homozygous tandem duplication within the gene encoding the beta-subunit of rod phosphodiesterase as a cause for autosomal recessive retinitis pigmentosa. Human Mutat. 1995; 5:228–234.
14. Danciger M, Blaney J, Gao YQ, et al. Mutations in the PDE6B gene in autosomal recessive retinitis pigmentosa. Genomics. 1995; 30:1–7. [PubMed: 8595886]
15. Danciger M, Heilbron V, Gao YQ, et al. A homozygous PDE6B mutation in a family with autosomal recessive retinitis pigmentosa. Mol Vis. 1996; 2:10. [PubMed: 9238087]
16. Valverde D, Solans T, Grinberg D, et al. A novel mutation in exon 17 of the beta-subunit of rod phosphodiesterase in two RP sisters of a consanguineous family. Human Genet. 1996; 97:35–38. [PubMed: 8557257]
17. Hmani-Aifa M, Benzina Z, Zulfiqar F, et al. Identification of two new mutations in the GPR98 and the PDE6B genes segregating in a Tunisian family. Eur J Human Genet. 2009; 17:474–482. [PubMed: 18854872]
18. Saga M, Mashima Y, Akeo K, et al. A novel homozygous Ile535Asn mutation in the rod cGMP phosphodiesterase beta-subunit gene in two brothers of a Japanese family with autosomal recessive retinitis pigmentosa. Curr Eye Res. 1998; 17:332–335. [PubMed: 9543643]
19. Ali S, Riazuddin SA, Shahzadi A, et al. Mutations in the beta-subunit of rod phosphodiesterase identified in consanguineous Pakistani families with autosomal recessive retinitis pigmentosa. Mol Vis. 2011; 17:1373–1380. [PubMed: 21655355]
20. Audo I, Tsang SH, Fu AD, et al. Autofluorescence imaging in a case of benign familial fleck retina. Arch Ophthalmol. 2007; 125:714–715. [PubMed: 17502520]
21. Tsui I, Chou CL, Palmer N, et al. Phenotype-genotype correlations in autosomal dominant retinitis pigmentosa caused by RHO, D190N. Curr Eye Res. 2008; 33:1014–1022. [PubMed: 19085385]
22. Gomes NL, Greenstein VC, Carlson JN, et al. A comparison of fundus autofluorescence and retinal structure in patients with Stargardt disease. Invest Ophthalmol Vis Sci. 2009; 50:3953–3959. [PubMed: 19324865]

23. Chen RW, Greenberg JP, Lazow MA, et al. Autofluorescence imaging and spectral-domain optical coherence tomography in incomplete congenital stationary night blindness and comparison with retinitis pigmentosa. Am J Ophthalmol. 2012; 153:143–154. e142. [PubMed: 21920492]
24. Duncker T, Tabacaru MR, Lee W, et al. Comparison of near-infrared and short-wavelength autofluorescence in retinitis pigmentosa. Invest Ophthalmol Vis Sci. 2013; 54:585–591. [PubMed: 23287793]
25. Lee TJ, Hwang JC, Chen RW, et al. The role of fundus autofluorescence in late-onset retinitis pigmentosa (LORP) diagnosis. Ophthalmic Genet. 201310.3109/13816810.2013.800891
26. Weber B, Riess O, Hutchinson G, et al. Genomic organization and complete sequence of the human gene encoding the beta-subunit of the cGMP phosphodiesterase and its localisation to 4p 16.3. Nucleic Acids Res. 1991; 19:6263–6268. [PubMed: 1720239]
27. Lisman J, Fain G. Support for the equivalent light hypothesis for RP. Nature Med. 1995; 1:1254–1255. [PubMed: 7489404]
28. Vallazza-Deschamps G, Cia D, Gong J, et al. Excessive activation of cyclic nucleotide-gated channels contributes to neuronal degeneration of photoreceptors. Eur J Neurosci. 2005; 22:1013–1022. [PubMed: 16176343]
29. Tsang SH, Tsui I, Chou CL, et al. A novel mutation and phenotypes in phosphodiesterase 6 deficiency. Am J Ophthalmol. 2008; 146:780–788. [PubMed: 18723146]
30. Jacobson SG, Sumaroka A, Aleman TS, et al. Evidence for retinal remodelling in retinitis pigmentosa caused by PDE6B mutation. Br J Ophthalmol. 2007; 91:699–701. [PubMed: 17446517]
31. Lima LH, Cella W, Greenstein VC, et al. Structural assessment of hyperautofluorescent ring in patients with retinitis pigmentosa. Retina. 2009; 29:1025–1031. [PubMed: 19584660]
32. Robson AG, Saihan Z, Jenkins SA, et al. Functional characterisation and serial imaging of abnormal fundus autofluorescence in patients with retinitis pigmentosa and normal visual acuity. Br J Ophthalmol. 2006; 90:472–479. [PubMed: 16547330]
33. Lima LH, Burke T, Greenstein VC, et al. Progressive constriction of the hyperautofluorescent ring in retinitis pigmentosa. Am J Ophthalmol. 2012; 153:718–727. e711–712. [PubMed: 22137208]
34. Mitamura Y, Aizawa S, Baba T, et al. Correlation between retinal sensitivity and photoreceptor inner/outer segment junction in patients with retinitis pigmentosa. Br J Ophthalmol. 2009; 93:126–127. [PubMed: 19098050]
35. Fishman GA, Gilbert LD, Fiscella RG, et al. Acetazolamide for treatment of chronic macular edema in retinitis pigmentosa. Arch Ophthalmol. 1989; 107:1445–1452. [PubMed: 2803090]
36. Neveling K, Collin RW, Gilissen C, et al. Next-generation genetic testing for retinitis pigmentosa. Human Mutat. 2012; 33:963–972.
37. Shanks ME, Downes SM, Copley RR, et al. Next-generation sequencing (NGS) as a diagnostic tool for retinal degeneration reveals a much higher detection rate in early-onset disease. Eur J Human Genet. 2013; 21:274–280. [PubMed: 22968130]
38. Audo I, Bujakowska KM, Leveillard T, et al. Development and application of a next-generation-sequencing (NGS) approach to detect known and novel gene defects underlying retinal diseases. Orphanet J Rare Diseases. 2012; 7:8. [PubMed: 22277662]
39. Bowne SJ, Sullivan LS, Koboldt DC, et al. Identification of disease-causing mutations in autosomal dominant retinitis pigmentosa (adRP) using next-generation DNA sequencing. Invest Ophthalmol Vis Sci. 2011; 52:494–503. [PubMed: 20861475]
40. Avila-Fernandez A, Cantalapiedra D, Aller E, et al. Mutation analysis of 272 Spanish families affected by autosomal recessive retinitis pigmentosa using a genotyping microarray. Mol Vis. 2010; 16:2550–2558. [PubMed: 21151602]

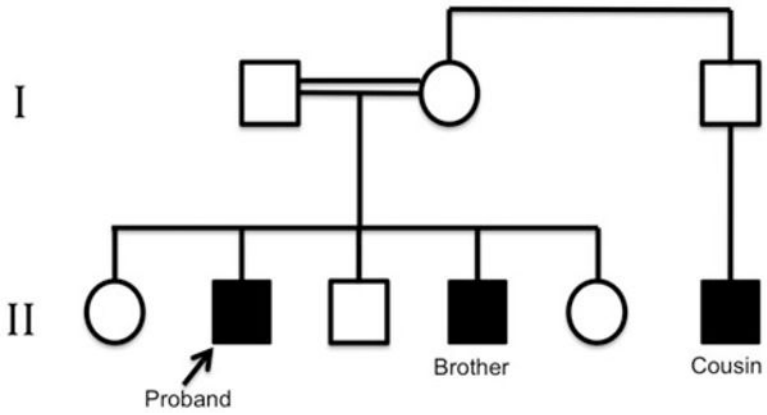

FIGURE 1.

Pedigree of the family shows the proband, his affected brother, and their affected cousin, who have homozygous c.1923_1969ins6del47 mutations. The mother, father, brother, and two sisters are heterozygous carriers. The parents are first cousins.

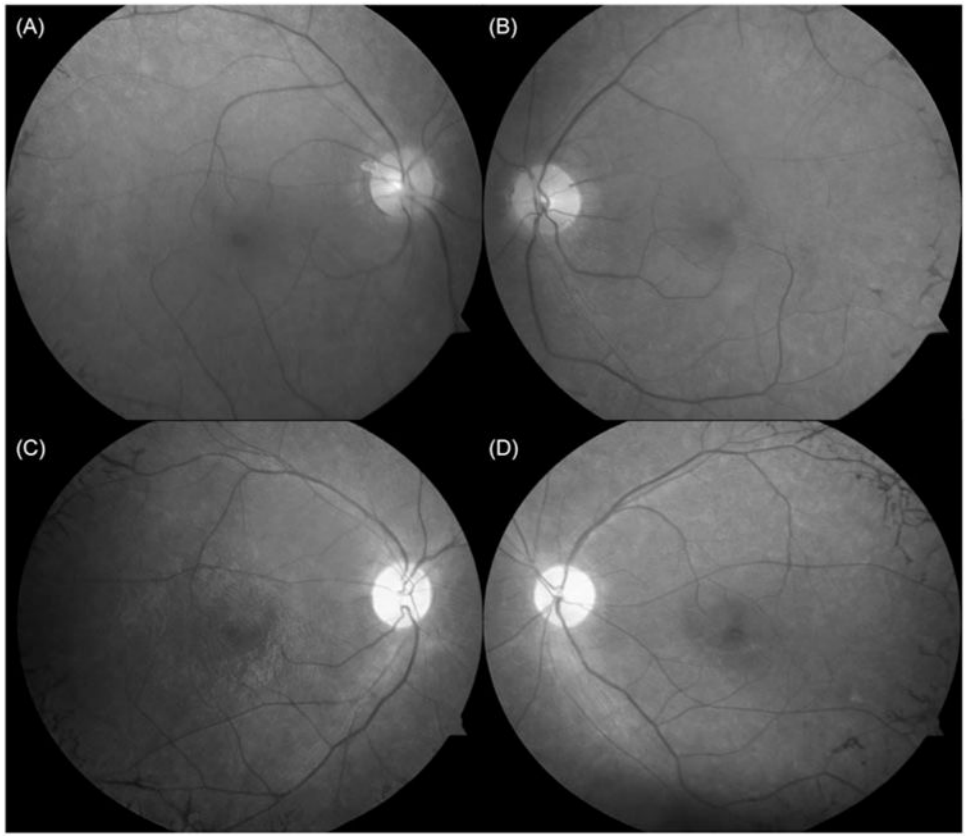

FIGURE 2.

Color fundus photographs from the proband and his affected brother show bone spicule intraretinal pigment migration, attenuated vessels, and optic disc drusen in the proband. (A, B) Proband OD, OS. (C, D) Affected brother OD, OS.

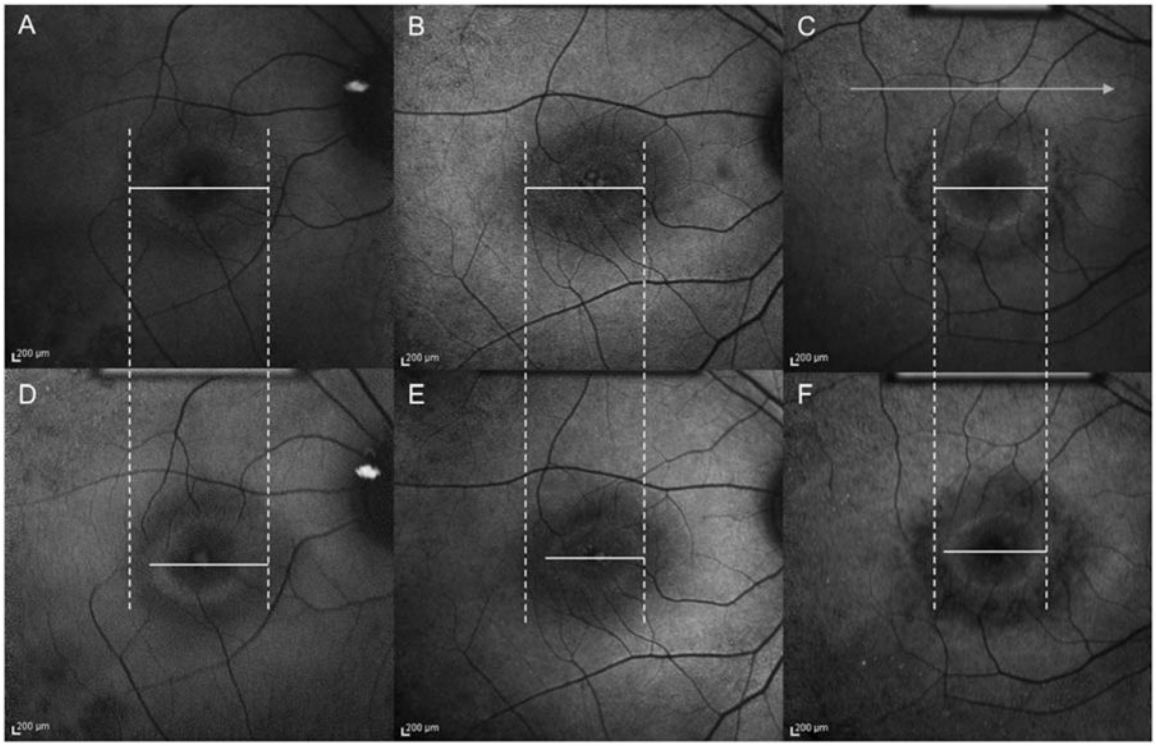

FIGURE 3.

FAF shows hyperautofluorescent ring constriction over time. White dotted lines mark width of ring outer border at first exam; white solid line denotes width of ring outer border at each exam. (A) Proband OD 5/2011. (B) Brother OD 8/2012. (C) Cousin OD 9/2010. (D) Proband OD 3/2013. (E) Brother OD 7/2013. (F) Cousin OD 10/2013.

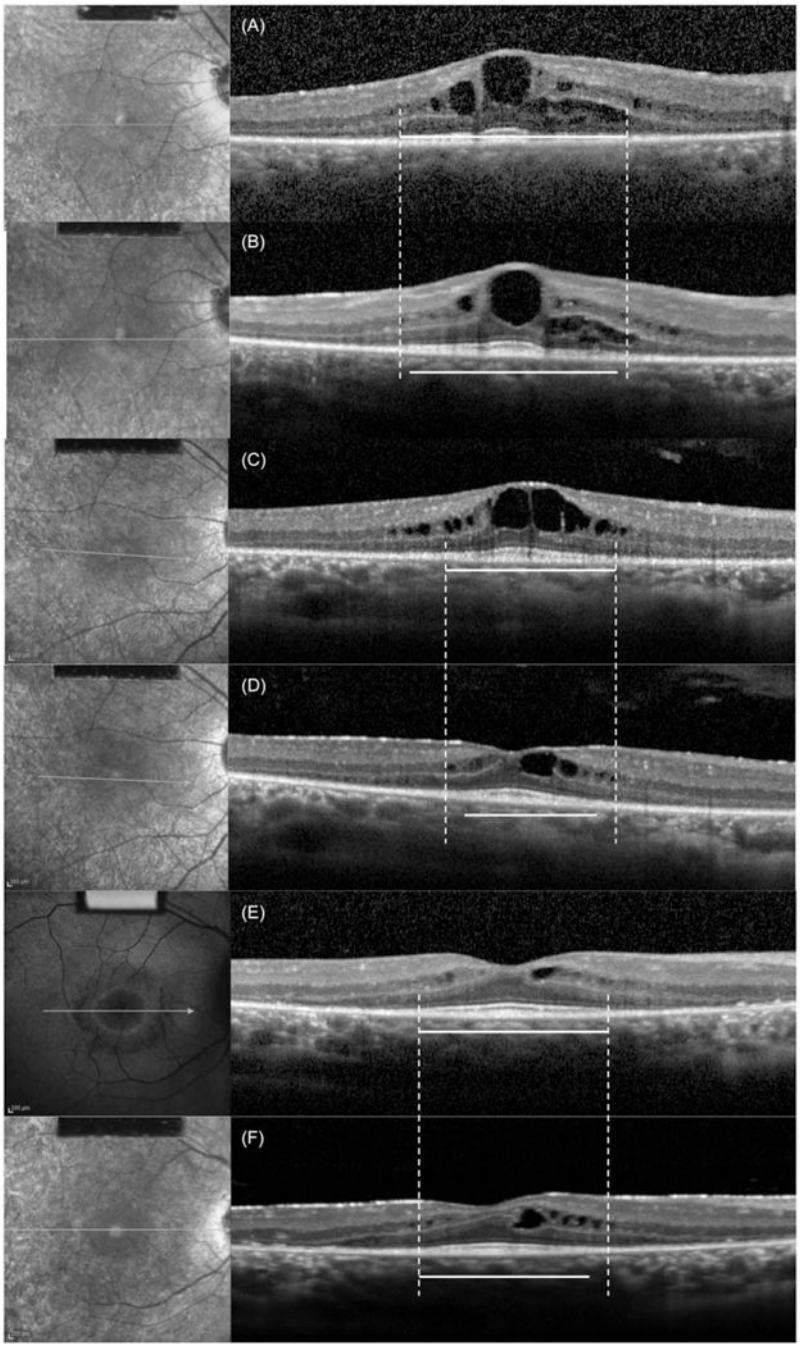

FIGURE 4.

SD-OCT shows reduction in length of the ellipsoid zone over time. White dotted lines mark length of ellipsoid zone at first exam; white solid line denotes length of ellipsoid zone at each exam. (A) Proband OD 5/2011. (B) Proband OD 3/2013. (C) Brother OD 8/2012. (D) Brother OD 7/2013. (E) Cousin OD 9/2010. (F) Cousin OD 10/2013.

TABLE 1

Patient demographics and clinical findings in the proband, his brother, and their cousin. The proband's first visit was in May 2011, and follow-up visit in March 2013. The brother's first visit was in August 2012, and follow-up visit in July 2013. The cousin's first visit was in September 2010, and follow-up visit in October 2013.

Family member	Age	RP onset age	BCVA first visit	BCVA follow-up visit
Proband	22	9	20/60 OU	20/30 OU
Brother	14	10	20/30 OU	20/20 OD
				20/25 OS
Cousin	21	9	20/80 OD	$20/25^{+2}$ OU
			$20/60^{-1}$ OS	